

# First observation of spin dichroism with deuterons up to 20 MeV in a carbon target

V. Baryshevsky\*, A. Rouba†

*Research Institute of Nuclear Problems, Bobruiskaya Str.11, 220050 Minsk, Belarus*

R. Engels, F. Rathmann, H. Seyfarth, H. Ströher, T. Ullrich

*Institut für Kernphysik, Forschungszentrum Jülich, Leo-Brandt-Str.1, 52425 Jülich, Germany*

C. Düweke, R. Emmerich, A. Imig, J. Ley, H. Paetz gen. Schieck, R. Schulze, G. Tenckhoff, C. Weske

*Institut für Kernphysik, Universität zu Köln, Zülpicher Str.77, D-50937 Köln, Germany*

M. Mikirtychians, A. Vassiliev  
PNPI, 188300 Gatchina, Russia

The first observation of the phenomenon of deuteron spin dichroism in the energy region of 6–20 MeV is described. Experimental values of this effect for deuterons after passage of an unpolarized carbon target are reported.

PACS numbers: 27.10.+h

## I. INTRODUCTION

It has been a longtime belief that the phenomena of rotation of the polarization plane and birefringence applies to only photons. The discovery of neutron spin precession in a polarized target due to the nuclear pseudomagnetic field [1]–[4] and subsequent analyses have shown that analogues of these effects exist not only for photons, but also for other particles [5, 6]. Thus, the optical effects caused by the anisotropy of matter represent only a special case of the coherent phenomena arising at the passage of polarized particles through matter.

The investigation of spin-dependent interactions of particles is an important part of the research programs to be carried out at storage rings, e.g. RHIC or COSY. The study of a number of phenomena in particle physics demands knowledge of imaginary and real parts of the forward scattering amplitude. Whereas the imaginary part, according to the optical theorem, can be found through the total scattering cross section, the real part may be obtained through the dispersion relations or by using the extrapolation of results from small-angle scattering. Thus, the phenomena of birefringence (spin rotation and oscillation) and spin dichroism (defined as the production of spin polarization in an unpolarized beam) of deuterons [5, 6] moving through homogeneous isotropic matter are of great interest. These phenomena allow the measurement of the real part of the spin-dependent forward scattering amplitude directly. Thus, a check of the dispersion relations on the basis of independent measurements of the imag-

inary and real part becomes possible. The confirmation of the existence of these effects would necessitate taking them into account in all experiments where particles with spins higher than 1/2 are scattered from polarized and unpolarized targets. Especially, their contribution to experiments in storage rings [7] and deuteron polarization measurements with thick targets [8] has to be considered. Particularly, the considered effect in the residual gas of a storage ring should be taken into account for precision EDM measurements [9].

The experiment analyzed in this paper has been devoted to the first attempt to measure spin dichroism, i. e. creation of tensor polarization in an unpolarized deuteron beam by unpolarized carbon targets. The experiment was carried out in the Institute of Nuclear Physics of the University of Cologne using the electrostatic HVEC tandem Van-de-Graaff accelerator with deuterons of up to 20 MeV. A  ${}^3\text{He}$  polarimeter, based upon the reaction  $d + {}^3\text{He} \rightarrow {}^4\text{He} + p$ , was used to measure polarization of transmitted deuterons.

## II. THEORY: ROTATION AND OSCILLATION OF DEUTERON SPIN IN UNPOLARIZED MATTER (BIREFRINGENCE AND SPIN DICHROISM)

According to [5, 6] the index of refraction for a deuteron (spin S=1) can be written as:

$$\hat{N} = 1 + \frac{2\pi\rho}{k^2}\hat{f}(0), \quad (1)$$

where  $\hat{f}(0) = Tr\hat{\rho}_J\hat{F}(0)$ ,  $\rho$  is the density of matter (the number of scatterers in  $1\text{ cm}^3$ ),  $k$  is the deuteron

\*E-mail: bar@inp.minsk.by; v\_baryshevsky@yahoo.com

†E-mail: rouba@inp.minsk.by

wave number,  $\hat{\rho}_J$  is the spin density matrix of the scatterers,  $\hat{F}(0)$  is the operator of the forward scattering amplitude acting in the combined spin space of the deuteron and scatterer spin  $\vec{J}$ .

For an unpolarized target  $\hat{f}(0)$  can be written as:

$$\hat{f}(0) = d + d_1 S_z^2. \quad (2)$$

where  $S_z$  is the z component of the deuteron spin operator. The axis of quantization  $z$  is directed along the particle wave vector  $\vec{k}$ . Considering only strong interactions, which are invariant to the parity transformation and time reversal, we may omit the terms containing  $S$  in odd degrees. Therefore, the refractive index for deuterons

$$\hat{N} = 1 + \frac{2\pi\rho}{k^2} (d + d_1 S_z^2) \quad (3)$$

depends on the deuteron spin orientation relative to the deuteron momentum.

The refractive index for a particle in the state, which is the eigenstate of the operator  $S_z$  of spin projection on the axis  $z$  is:

$$\hat{N} = 1 + \frac{2\pi\rho}{k^2} (d + d_1 m^2), \quad (4)$$

where  $m$  is the magnetic quantum number.

According to Eq.(4), the refractive indices for the states with  $m = +1$  and  $m = -1$  are the same, while those for  $m = \pm 1$  and  $m = 0$  are different ( $\Re N(\pm 1) \neq \Re N(0)$  and  $\Im N(\pm 1) \neq \Im N(0)$ ). This can be obviously explained as follows (see Fig.1): the shape of a deuteron in the ground state is non-spherical. Therefore, the scattering cross-section  $\sigma_{\parallel}$  for a deuteron with  $m = \pm 1$  (deuteron spin is parallel to its momentum  $\vec{k}$ ) differs from the scattering cross-section  $\sigma_{\perp}$  for a deuteron with  $m = 0$ :

$$\sigma_{\parallel} \neq \sigma_{\perp} \Rightarrow \Im f_{\parallel}(0) = \frac{k}{4\pi} \sigma_{\parallel} \neq \Im f_{\perp}(0) = \frac{k}{4\pi} \sigma_{\perp}. \quad (5)$$

According to the dispersion relation  $\Re f(0) \sim \Phi(\Im f(0))$ , then  $\Re f_{\perp}(0) \neq \Re f_{\parallel}(0)$ .

From the above it follows that deuteron spin dichroism appears even when a deuteron passes through an unpolarized target: due to different absorption the initially unpolarized beam acquires polarization or, yet more precisely, alignment.

Let us consider the behavior of the deuteron spin in a target. The spin state of the deuteron is described by its vector and tensor polarization ( $\vec{p} = \langle \vec{S} \rangle$  and  $p_{ik} = \langle Q_{ik} \rangle$ , respectively). When the deuteron moves in matter its vector and tensor polarization appears changed. To calculate  $\vec{p}$  and  $p_{ik}$  one need to know the explicit form of the deuteron spin wave function  $\psi$

The wave function of the deuteron that has passed the distance  $z$  inside the target is:

$$\psi(z) = \exp\left(ik\hat{N}z\right) \psi_0, \quad (6)$$

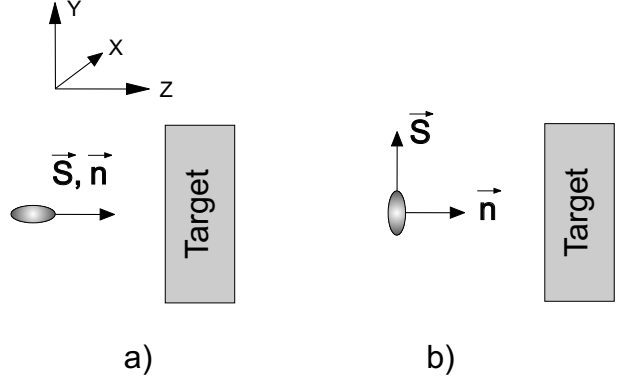


Fig. 1: Two possible orientation of vectors  $\vec{S}$  and  $\vec{n} = \frac{\vec{k}}{k}$ :  
a)  $\vec{S} \parallel \vec{n}$ ; b)  $\vec{S} \perp \vec{n}$

where  $\psi_0$  is the wave function of the deuteron before entering the target. The wave function  $\psi$  can be expressed as a superposition of the basic spin functions  $\chi_m$ , which are the eigenfunctions of the operators  $\hat{S}^2$  and  $\hat{S}_z$  ( $\hat{S}_z \chi_m = m \chi_m$ ):

$$\psi = \sum_{m=\pm 1,0} a^m \chi_m. \quad (7)$$

Therefore,

$$\Psi = \begin{pmatrix} a^1 \\ a^0 \\ a^{-1} \end{pmatrix} = \begin{pmatrix} ae^{i\delta_1} e^{ikN_1 z} \\ be^{i\delta_0} e^{ikN_0 z} \\ ce^{i\delta_{-1}} e^{ikN_{-1} z} \end{pmatrix} = \begin{pmatrix} ae^{i\delta_1} e^{ikN_1 z} \\ be^{i\delta_0} e^{ikN_0 z} \\ ce^{i\delta_{-1}} e^{ikN_1 z} \end{pmatrix}, \quad (8)$$

(according to the above  $N_1 = N_{-1}$ ).

Suppose the plane ( $yz$ ) coincides with the plane formed by the initial deuteron vector polarization  $\vec{p}_0 \neq 0$  and the momentum  $\vec{k}$  of the deuteron. In this case  $\delta_1 - \delta_0 = \delta_0 - \delta_{-1} = \frac{\pi}{2}$ , and the components of the polarization vector at  $z = 0$  are  $p_x = 0$ ,  $p_y \neq 0$ , and  $p_z \neq 0$ .

The components of the vector polarization  $\vec{p} = \langle \vec{S} \rangle = \frac{\langle \Psi | \vec{S} | \Psi \rangle}{\langle \Psi | \Psi \rangle}$  inside the target are:

$$\begin{aligned} p_x &= \frac{\sqrt{2}e^{-\frac{1}{2}\rho(\sigma_0+\sigma_1)z}b(a-c)\sin\left(\frac{2\pi\rho}{k}\Re d_1 z\right)}{\langle \Psi | \Psi \rangle}, \\ p_y &= \frac{\sqrt{2}e^{-\frac{1}{2}\rho(\sigma_0+\sigma_1)z}b(a+c)\cos\left(\frac{2\pi\rho}{k}\Re d_1 z\right)}{\langle \Psi | \Psi \rangle}, \\ p_z &= \frac{e^{\rho\sigma_1 z}(a^2 - c^2)}{\langle \Psi | \Psi \rangle}. \end{aligned} \quad (9)$$

Similarly, the components of the tensor polarization  $\hat{Q}_{ij} = \frac{3}{2} \left( \hat{S}_i \hat{S}_j + \hat{S}_j \hat{S}_i - \frac{4}{3} \delta_{ij} \right)$  are expressed as:

$$\begin{aligned}
p_{xx} &= \frac{-\frac{1}{2}(a^2 + c^2)e^{-\rho\sigma_1 z} + b^2e^{-\rho\sigma_0 z} - 3ace^{-\rho\sigma_1 z}}{\langle\Psi|\Psi\rangle}, \\
p_{yy} &= \frac{-\frac{1}{2}(a^2 + c^2)e^{-\rho\sigma_1 z} + b^2e^{-\rho\sigma_0 z} + 3ace^{-\rho\sigma_1 z}}{\langle\Psi|\Psi\rangle}, \\
p_{zz} &= \frac{(a^2 + c^2)e^{-\rho\sigma_1 z} - 2b^2e^{-\rho\sigma_0 z}}{\langle\Psi|\Psi\rangle}, \\
p_{xy} &= 0, \\
p_{xz} &= \frac{\frac{3}{\sqrt{2}}e^{-\frac{1}{2}\rho(\sigma_0+\sigma_1)z}b(a+c)\sin\left(\frac{2\pi\rho}{k}\Re d_1 z\right)}{\langle\Psi|\Psi\rangle}, \\
p_{yz} &= \frac{\frac{3}{\sqrt{2}}e^{-\frac{1}{2}\rho(\sigma_0+\sigma_1)z}b(a-c)\cos\left(\frac{2\pi\rho}{k}\Re d_1 z\right)}{\langle\Psi|\Psi\rangle}, \quad (10)
\end{aligned}$$

where  $\langle\Psi|\Psi\rangle = (a^2 + c^2)e^{-\rho\sigma_1 z} + b^2e^{-\rho\sigma_0 z}$ ,  $\sigma_0 = \frac{4\pi}{k}\Im f_0$ ,  $\sigma_1 = \frac{4\pi}{k}\Im f_1$ ,  $f_0 = d$ ,  $f_1 = d + d_1$ .

According to (9,10) the spin rotation occurs when the angle between the polarization vector  $\vec{p}$  and momentum  $\vec{k}$  of the particle differs from  $\frac{\pi}{2}$ .

For example, when  $\Re d_1 > 0$ , the angle between the polarization vector and momentum is acute and the spin rotates left-hand around the momentum direction, whereas the obtuse angle between the polarization vector and momentum gives rise to the right-hand spin rotation.

When the polarization vector and momentum are perpendicular (transversely polarized particle), then the components of the vector polarization at  $z = 0$  are:  $p_x = 0$ ,  $p_y \neq 0$ , and  $p_z = 0$ . In this case  $a = c$  and the dependance of the vector polarization on  $z$  can be expressed as:

$$\begin{aligned}
p_x &= 0, \\
p_y &= \frac{\sqrt{2}e^{-\frac{1}{2}\rho(\sigma_0+\sigma_1)z}2ba\cos\left(\frac{2\pi\rho}{k}\Re d_1 z\right)}{\langle\Psi|\Psi\rangle}, \\
p_z &= 0, \\
p_{xx} &= \frac{-4a^2e^{-\rho\sigma_1 z} + b^2e^{-\rho\sigma_0 z}}{\langle\Psi|\Psi\rangle}, \quad (11) \\
p_{yy} &= \frac{2a^2e^{-\rho\sigma_1 z} + b^2e^{-\rho\sigma_0 z}}{\langle\Psi|\Psi\rangle}, \\
p_{zz} &= \frac{2a^2e^{-\rho\sigma_1 z} - 2b^2e^{-\rho\sigma_0 z}}{\langle\Psi|\Psi\rangle}, \\
p_{xz} &= \frac{\frac{3}{\sqrt{2}}e^{-\frac{1}{2}\rho(\sigma_0+\sigma_1)z}2ab\sin\left(\frac{2\pi\rho}{k}\Re d_1 z\right)}{\langle\Psi|\Psi\rangle}, \\
p_{yz} &= 0.
\end{aligned}$$

According to (12) the vector and tensor polarization oscillate when a transversely polarized deuteron passes through matter.

### III. SPIN ROTATION AND OSCILLATION AND SPIN DICHROISM OF A 20 MEV STORED DEUTERON BEAM

Let us consider the 20 MeV deuteron beam passing through unpolarized matter (this energy is typical for low-energy accelerators). The density matrix for the deuteron beam before the target can be written as follows:

$$\begin{aligned}
\hat{\rho}_0 &= \frac{\hat{I}}{3} + \frac{1}{2}\left(\vec{p}_x\hat{S}_x + \vec{p}_y\hat{S}_y + \vec{p}_z\hat{S}_z\right) \\
&+ \frac{2}{9}\left(p_{xy}\hat{Q}_{xy} + p_{xz}\hat{Q}_{xz} + p_{yz}\hat{Q}_{yz}\right) \\
&+ \frac{1}{9}\left(p_{xx}\hat{Q}_{xx} + p_{yy}\hat{Q}_{yy} + p_{zz}\hat{Q}_{zz}\right). \quad (12)
\end{aligned}$$

Using (8) we can express the density matrix of the deuteron beam in the target as:

$$\begin{aligned}
\hat{\rho} &= \begin{pmatrix} e^{ikzN_1} & 0 & 0 \\ 0 & e^{ikN_0 z} & 0 \\ 0 & 0 & e^{ikN_1 z} \end{pmatrix} \hat{\rho}_0 \times \\
&\quad \begin{pmatrix} e^{-ikN_1^* z} & 0 & 0 \\ 0 & e^{-ikN_0^* z} & 0 \\ 0 & 0 & e^{-ikN_1^* z} \end{pmatrix} \quad (13)
\end{aligned}$$

then

$$\vec{p} = \langle\vec{S}\rangle = \frac{\text{Tr}(\hat{\rho}\hat{S})}{\text{Tr}(\hat{\rho})}, \quad p_{ik} = \langle Q_{ik} \rangle = \frac{\text{Tr}(\hat{\rho}\hat{Q}_{ik})}{\text{Tr}(\hat{\rho})}$$

where  $i, k = x, y, z$ .

Suppose  $p_{x,0}$ ,  $p_{y,0}$ ,  $p_{z,0}$ ,  $p_{xx,0}$ ,  $p_{yy,0}$ ,  $p_{zz,0}$ ,  $p_{xy,0}$ ,  $p_{xz,0}$ ,  $p_{yz,0}$  are the components of the deuteron vector and tensor polarization before entering the target then the vector and tensor polarization of the deuteron inside the target can be expressed using the first-order approximation  $e^{ikz(N_1 - N_1^*)} \approx 1 + ikz(N_1 - N_1^*)$  as:

$$\begin{aligned}
p_x &= \frac{[1 - \frac{1}{2}\rho z(\sigma_0 + \sigma_1)]p_{x,0} + \frac{4}{3}\frac{\pi\rho z}{k}\Re d_1 p_{zy,0}}{\text{Tr}\hat{\rho}\hat{I}}, \\
p_y &= \frac{[1 - \frac{1}{2}\rho z(\sigma_0 + \sigma_1)]p_{y,0} - \frac{4}{3}\frac{\pi\rho z}{k}\Re d_1 p_{zx,0}}{\text{Tr}\hat{\rho}\hat{I}}, \\
p_z &= \frac{(1 - \rho\sigma_1 z)p_{z,0}}{\text{Tr}\hat{\rho}\hat{I}}, \\
p_{xx} &= \frac{(1 - \rho\sigma_1 z)p_{xx,0} + \frac{1}{3}\rho z(\sigma_1 - \sigma_0) - \frac{1}{3}\rho z(\sigma_1 - \sigma_0)p_{zz,0}}{\text{Tr}\hat{\rho}\hat{I}}, \\
p_{yy} &= \frac{(1 - \rho\sigma_1 z)p_{yy,0} + \frac{1}{3}\rho z(\sigma_1 - \sigma_0) - \frac{1}{3}\rho z(\sigma_1 - \sigma_0)p_{zz,0}}{\text{Tr}\hat{\rho}\hat{I}}, \\
p_{zz} &= \frac{[1 - \frac{1}{3}\rho z(2\sigma_0 + \sigma_1)]p_{zz,0} - \frac{2}{3}\rho z(\sigma_1 - \sigma_0)}{\text{Tr}\hat{\rho}\hat{I}}, \\
p_{xy} &= \frac{(1 - \rho\sigma_1 z)p_{xy,0}}{\text{Tr}\hat{\rho}\hat{I}}, \quad (14)
\end{aligned}$$

$$\begin{aligned} p_{xz} &= \frac{[1 - \frac{1}{2}\rho z(\sigma_0 + \sigma_1)] p_{xz,0} + 3\frac{\pi\rho z}{k} \Re d_1 p_{y,0}}{Tr \hat{\rho} \hat{I}}, \\ p_{yz} &= \frac{[1 - \frac{1}{2}\rho z(\sigma_0 + \sigma_1)] p_{yz,0} - 3\frac{\pi\rho z}{k} \Re d_1 p_{x,0}}{Tr \hat{\rho} \hat{I}}, \end{aligned}$$

where  $Tr \hat{\rho} \hat{I} = 1 - \frac{\rho z}{3}(2\sigma_1 + \sigma_0) - \frac{\rho z}{3}(\sigma_1 - \sigma_0)p_{zz,0}$ .

If the beam is initially unpolarized ( $p_{x,0} = p_{y,0} = p_{z,0} = p_{xx,0} = p_{yy,0} = p_{zz,0} = p_{xy,0} = p_{xz,0} = p_{yz,0} = 0$ ) then after passing through the unpolarized target of thickness  $z$  the deuteron beam acquires the tensor polarization:

$$\begin{aligned} p_{zz} &\approx -\frac{2}{3}\rho z(\sigma_1 - \sigma_0), \\ p_{xx} = p_{yy} &\approx \frac{1}{3}\rho z(\sigma_1 - \sigma_0). \end{aligned} \quad (15)$$

The tensor polarization can be expressed by dichroism  $G$  of the unpolarized target:

$$p_{zz} \approx -\frac{4}{3}G, \quad p_{xx} = p_{yy} \approx \frac{2}{3}G, \quad (16)$$

where

$$G = \frac{I_0 - I_{\pm}}{I_0 + I_{\pm}} = \frac{\rho z}{2}(\sigma_1 - \sigma_0), \quad (17)$$

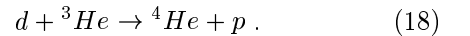
$I_0$  is the intensity of the deuteron beam after the target if the deuteron beam before the target is in the spin state  $m = 0$  and, similarly,  $I_{\pm}$  is the intensity of the deuteron beam after the target if the deuteron beam before the target is in the spin state  $m = \pm 1$ .

Let us evaluate the angle of spin rotation and dichroism of a 20 MeV deuteron beam in an unpolarized carbon target using the above formulas: suppose the target density  $\rho \approx 10^{23} \text{ cm}^{-3}$ , the target thickness  $z \approx 0.1 \text{ cm}$ ,  $\Re d_1 \approx 6 \cdot 10^{-13} \text{ cm}$ ,  $\sigma_1 - \sigma_0 \approx -10^{-25} \text{ cm}^2$  then the angle of rotation (the magnitude of oscillation phase) is  $\varphi = \frac{2\pi\rho}{k} \Re d_1 z \sim 10^{-3} \text{ rad}$  and dichroism is  $G \sim 10^{-2}$ .

The above evaluation considers only the non-spherical shape of a deuteron in the ground state, however an additional correction may occur when considering the spin-spin and Coulomb interactions at low energies. Moreover, the eikonal formalism [10] can not be applied to the low energy deuterons because the wavelength of a 20 MeV deuteron is compared with the nucleus size. Nevertheless, when suppose that the S-wave contributes the most to the scattering of a deuteron with the energy  $< 20 \text{ MeV}$  by a nucleus, then consideration shows that the difference  $(\sigma_1 - \sigma_0)$  (and hence, dichroism  $G$ ) has the same magnitude, while the sign is opposite.

#### IV. THE EXPERIMENT FOR DETECTION OF DEUTERON SPIN DICHROISM WITH A ${}^3\text{He}$ - POLARIMETER

The experiment for the detection of spin dichroism of deuterons in a carbon target was carried out at the accelerator of the Institute of Nuclear Physics of Cologne University. The existing  ${}^3\text{He}$  polarimeter of the experimental installation was used. The purpose was to measure all components of the deuteron vector and tensor polarization via anisotropies of the protons outgoing from the nuclear reaction [12, 13]



The polarimeter has four detectors at  $24.5^\circ$  polar angles in addition to the fifth detector measuring the emitted protons in the forward direction (at  $0^\circ$ ). This detector is sensitive only to the  $p_{zz}$ -component of the tensor polarization [13].

Let us briefly describe the measurement procedure. The most general form for the cross section of a parity conserving reaction induced by polarized spin 1 particle is [12]:

$$\begin{aligned} I(\theta, \varphi) &= I_0(\theta) \left[ 1 + \frac{3}{2}p_y A_y(\theta) \right. \\ &+ \frac{2}{3}p_{xz} A_{xz}(\theta) + \frac{1}{3}p_{xx} A_{xx}(\theta) \\ &\left. + \frac{1}{3}p_{yy} A_{yy}(\theta) + \frac{1}{3}p_{zz} A_{zz}(\theta) \right], \end{aligned} \quad (19)$$

where we use the projectile helicity coordinate system to describe scattering or reactions induced by polarized spin 1 particles. In this coordinate system the axis of quantization ( $z$  axis) is taken along the direction of the projectile motion  $\vec{k}$ ; the  $y$  axis is taken along  $\vec{k} \times \vec{k}'$ , where  $\vec{k}'$  represents the direction of scattered particle or reaction product motion; and the  $x$  axis is chosen to form a right-handed coordinate system,  $\theta$  is the angle between  $\vec{k}$  and  $\vec{k}'$ , and  $A$  is the analyzing power of the reaction. The incident beam

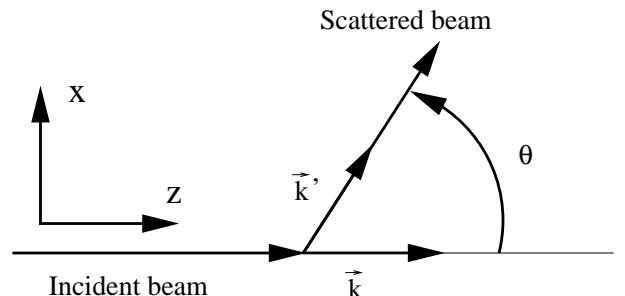


Fig. 2: The system of coordinates.

may have vector polarization components  $p_x$ ,  $p_y$  and  $p_z$ , but because of parity conservation the reaction is sensitive only to the vector component normal to the scattering plane. Similarly, although the incident

beam may contain all six tensor polarization components  $p_{xy}$ ,  $p_{yz}$ ,  $p_{xz}$ ,  $p_{xx}$ ,  $p_{yy}$  and  $p_{zz}$ , the reaction is sensitive, again because of parity, only to those terms indicated in equation (19). The diagonal elements of the tensor polarization meet the trace relation:

$$p_{xx} + p_{yy} + p_{zz} = 0. \quad (20)$$

Similarly, for the analyzing power components:

$$A_{xx} + A_{yy} + A_{zz} = 0. \quad (21)$$

Thus, only four of the five analyzing tensors that appear in (19) are independent.

The expression of equation (19) implies scattering to the left, if  $\vec{k} \times \vec{k}'$  defines the 'up' direction. If we define the azimuthal angle,  $\varphi$ , to be the angle between the plane containing both  $\vec{k} \times \vec{k}'$  and  $\vec{k}$ , and some fixed reference plane, which also contains  $\vec{k}$ , the most general possible azimuthal dependence for the cross section is:

$$\begin{aligned} I(\theta, \varphi) &= I_0(\theta) \times \\ &\times \left\{ 1 + \frac{3}{2}(p_{x'} \sin \varphi + p_{y'} \cos \varphi) A_y(\theta) \right. \\ &+ \frac{2}{3}(p_{x'z'} \cos \varphi - p_{y'z'} \sin \varphi) A_{xz}(\theta) \\ &+ \frac{1}{6}[(p_{x'z'} - p_{y'y'}) \cos 2\varphi - 2p_{x'y'} \sin 2\varphi] \times \\ &\times \left. [A_{xx}(\theta) - A_{yy}(\theta)] + \frac{1}{2}p_{z'z'} A_{zz}(\theta) \right\} \quad (22) \end{aligned}$$

The frame in terms of which the beam polarization is described ( $x'$ ,  $y'$ ,  $z'$ ) is defined according to [12]: suppose the beam has components of the vector polarization  $p_{x'}$ ,  $p_{y'}$ ,  $p_{z'}$ , where  $z'$  is along the beam direction and  $y'$  is chosen in a way that is natural for the polarized beam. For example, if the beam is prepared by a polarized ion source,  $y'$  is chosen so that its polarization axis of symmetry lies in the  $(y', z')$  plane with positive  $y'$ ; if it is prepared by scattering,  $y'$  is chosen along  $\vec{k} \times \vec{k}'$  for scattering. Fig.3 shows the relation between  $(x', y', z')$  (the beam coordinate system) and  $(x, y, z)$  (the analyzer coordinate system).

Using (22) we can express the number of events registered by the detectors of the  ${}^3\text{He}$ -polarimeter:  $L$  corresponds to the left detector ( $\theta = 24.5^\circ$ ,  $\varphi = 0^\circ$ ),  $R$ ,  $U$ ,  $D$  and  $F$  are for the right ( $\theta = 24.5^\circ$ ,  $\varphi = 180^\circ$ ), top ( $\theta = 24.5^\circ$ ,  $\varphi = 270^\circ$ ), bottom ( $\theta = 24.5^\circ$ ,  $\varphi = 90^\circ$ ) and forward ( $\theta = 0^\circ$ ) detectors, respectively.

$$\begin{aligned} L &= Nn\Omega_L EI_0(24.5^\circ) \times \\ &\times \left\{ 1 + \frac{3}{2}p_{y'} A_y(24.5^\circ) + \frac{2}{3}p'_x z' A_{xz}(24.5^\circ) \right. \\ &+ \frac{1}{6}(p_{x'z'} - p_{y'y'}) [A_{xx}(24.5^\circ) - A_{yy}(24.5^\circ)] \\ &\left. + \frac{1}{2}p_{z'z'} A_{zz}(24.5^\circ) \right\}; \end{aligned}$$

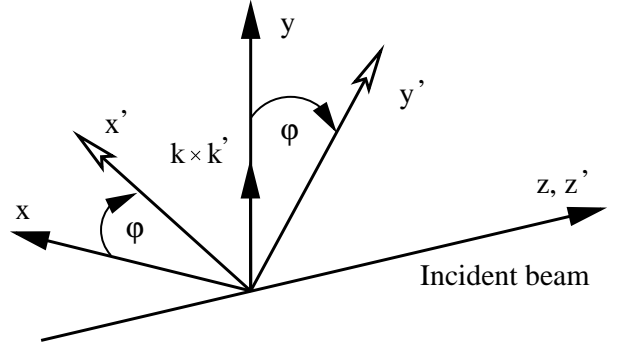


Fig. 3: Relation between the projectile helicity frame ( $x$ ,  $y$ ,  $z$ ) and the frame in terms of which the beam polarization is described ( $x'$ ,  $y'$ ,  $z'$ ). For left scattering ( $\varphi = 0$ ) these frames coincide.

$$\begin{aligned} R &= Nn\Omega_R EI_0(24.5^\circ) \times \\ &\times \left\{ 1 - \frac{3}{2}p_{y'} A_y(24.5^\circ) - \frac{2}{3}p'_x z' A_{xz}(24.5^\circ) \right. \\ &+ \frac{1}{6}(p_{x'z'} - p_{y'y'}) [A_{xx}(24.5^\circ) - A_{yy}(24.5^\circ)] \\ &\left. + \frac{1}{2}p_{z'z'} A_{zz}(24.5^\circ) \right\}; \\ U &= Nn\Omega_U EI_0(24.5^\circ) \times \\ &\times \left\{ 1 - \frac{3}{2}p_{y'} A_y(24.5^\circ) + \frac{2}{3}p'_x z' A_{xz}(24.5^\circ) \right. \\ &- \frac{1}{6}(p_{x'z'} - p_{y'y'}) [A_{xx}(24.5^\circ) - A_{yy}(24.5^\circ)] \\ &\left. + \frac{1}{2}p_{z'z'} A_{zz}(24.5^\circ) \right\}; \\ D &= Nn\Omega_D EI_0(24.5^\circ) \times \\ &\times \left\{ 1 + \frac{3}{2}p_{y'} A_y(24.5^\circ) - \frac{2}{3}p'_x z' A_{xz}(24.5^\circ) \right. \\ &- \frac{1}{6}(p_{x'z'} - p_{y'y'}) [A_{xx}(24.5^\circ) - A_{yy}(24.5^\circ)] \\ &\left. + \frac{1}{2}p_{z'z'} A_{zz}(24.5^\circ) \right\}; \\ F &= Nn\Omega_F EI_0(0^\circ) \left[ 1 + \frac{1}{2}p_{z'z'} A_{zz}(0^\circ) \right], \end{aligned}$$

where  $N$  is the surface density of the  ${}^3\text{He}$  target in  $\text{cm}^{-2}$ ,  $n$  is the number of incident deuterons,  $\Omega$  is the solid angle, and  $E$  is the efficiency of each detector.

The scheme of the polarimeter [13] is shown in Fig.4, Figs. 5-8 display typical spectrums of detected protons produced by deuterons in the  ${}^3\text{He}$  cell and analyzing power for the side and forward detectors.

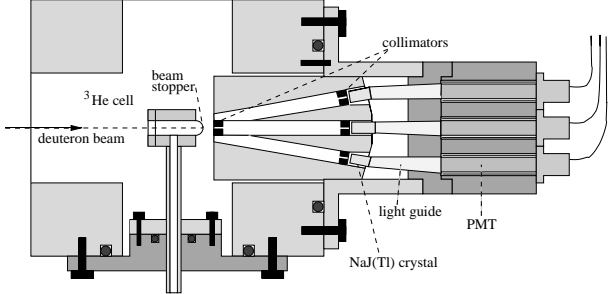


Fig. 4:  $^3\text{He}$ -Polarimeter.

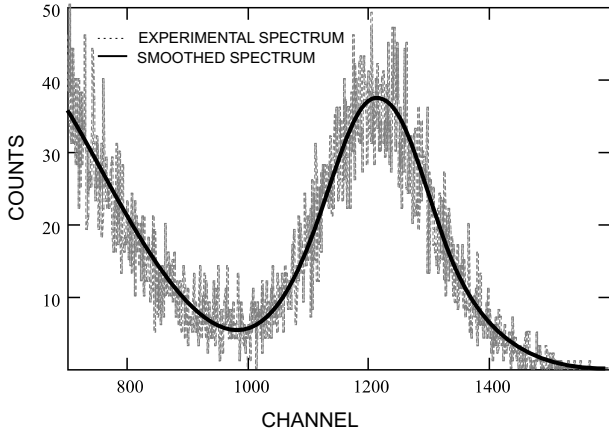


Fig. 5: Energy spectrum of protons registered by one side detector, produced by deuterons with an initial energy of 16.2 MeV after passing through the  $151 \text{ mg/cm}^2$  carbon target.

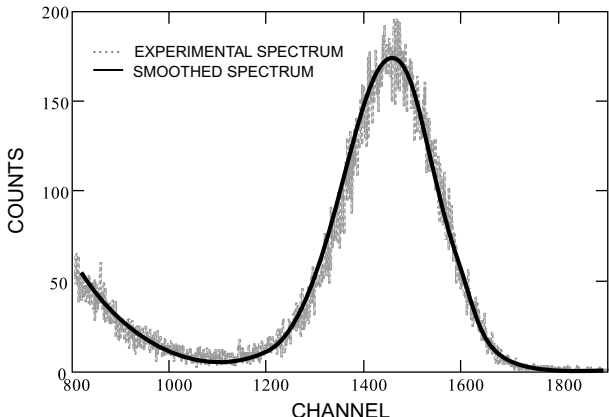


Fig. 6: Energy spectrum of protons registered by the forward detector, produced by deuterons with an initial energy of 16.2 MeV after passing through the  $151 \text{ mg/cm}^2$  carbon target.

## V. DISCUSSION: GENERAL APPROACH TO SPIN DICHROISM MEASUREMENT IN VIEW OF $^3\text{He}$ -POLARIMETER FEATURES

Dichroism and tensor polarization of the deuteron beam passing through the carbon target was eval-

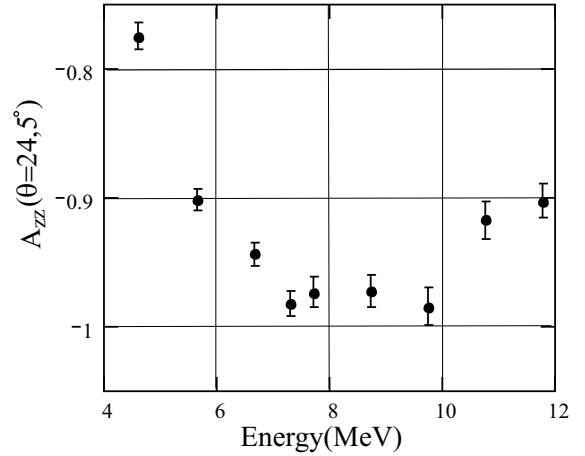


Fig. 7: Analyzing power for the side detectors.

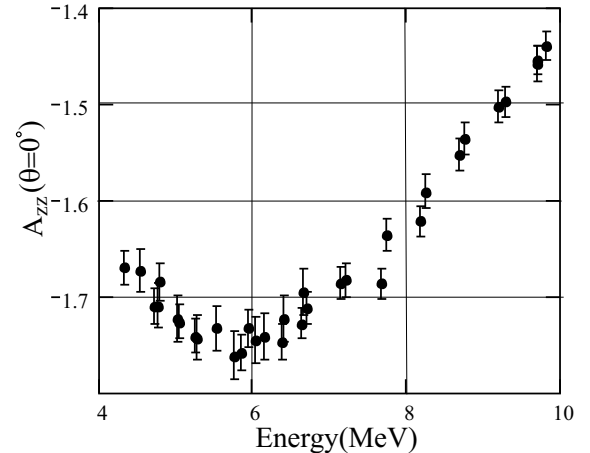


Fig. 8: Analyzing power for the forward detector.

uated in the previous sections as  $\sim 10^{-2}$ . Therefore, the number of particles detected when deuteron beam passed through the target is two orders less than the number of particles detected without a target.

During the experiment several issues arose. The first is associated with the dependence of the detector count rate on beam focusing.

The beam crossover with no target was small and it could cross the helium cell in different places resulting in the variation in solid angle ratios between different detectors. Thus, individual numbers of events registered by each detector could vary in about 5 %.

Incomplete suppression of secondary electrons in the polarimeter caused the second issue: the number of counts for the equal charge also substantially depended on focusing.

The differential cross section of the reaction  $d + ^3\text{He} \rightarrow ^4\text{He} + p$  strongly depends on energy as

it is shown in Fig. 9,10 [14]. For these reasons, it

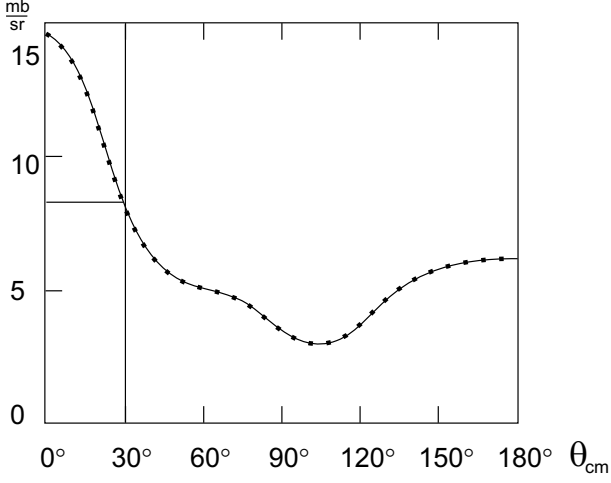


Fig. 9: Differential cross section of the  ${}^3\text{He}(\text{d}, \text{p}){}^4\text{He}$  reaction at 6 MeV.

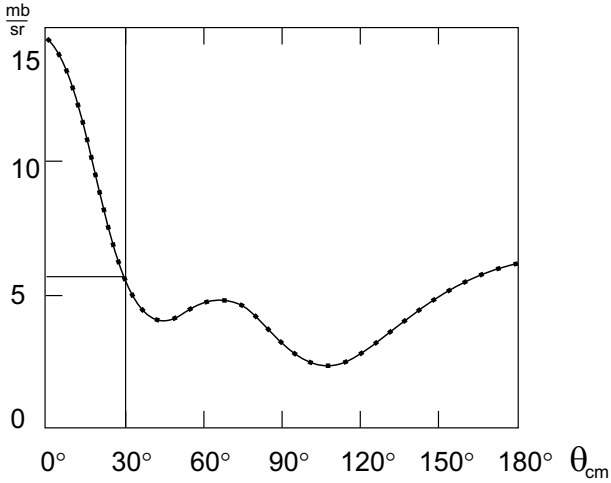


Fig. 10: Differential cross section of the  ${}^3\text{He}(\text{d}, \text{p}){}^4\text{He}$  reaction at 8 MeV.

was impossible to calibrate the detectors accurately. Besides, the tensor polarization could be found only approximately. In the following experiment the measurement will be improved. It is necessary to choose such combinations of  $L, R, U, D, F$  with and without a target so that the results can become maximally insensitive to solid-angle variations. Let us designate by  $L_t, R_t, U_t, D_t, F_t$  the number of the registered particles with a target, and  $L, R, U, D, F$  without. According to Eqs. (14),(15), after the target the beam has only diagonal components of the tensor polarization  $p_{zz}, p_{xx}, p_{yy}$ , but as  $p_{xx} = p_{yy}$ , we obtain:

$$\begin{aligned} L_t &= Nn_t \Omega_L EI_0(24.5^\circ) [1 + \frac{1}{2} p_{zz'} A_{zz}(24.5^\circ)] \\ L &= Nn \Omega_L EI_0(24.5^\circ) \end{aligned}$$

$$\begin{aligned} R_t &= Nn \Omega_R EI_0(24.5^\circ) \\ U_t &= Nn_t \Omega_U EI_0(24.5^\circ) [1 + \frac{1}{2} p_{zz'} A_{zz}(24.5^\circ)] \\ U &= Nn \Omega_U EI_0(24.5^\circ) \\ D_t &= Nn_t \Omega_D EI_0(24.5^\circ) [1 + \frac{1}{2} p_{zz'} A_{zz}(24.5^\circ)] \\ D &= Nn \Omega_D EI_0(24.5^\circ) \\ F_t &= Nn_t \Omega_F EI_0(0^\circ) [1 + \frac{1}{2} p_{zz'} A'_{zz}(0^\circ)] \\ F &= Nn \Omega_F EI_0(0^\circ) \end{aligned}$$

The relevant combinations used in the data reduction – their variation in this case was about 0.2% – were therefore:

$$\frac{L + R + U + D}{F} = \frac{(\Omega_L + \Omega_R + \Omega_U + \Omega_D) I_0(24.5^\circ)}{\Omega_F I_0(0^\circ)} \quad (23)$$

$$\begin{aligned} &\frac{L_t + R_t + U_t + D_t}{F_t} \\ &= \frac{(\Omega_L + \Omega_R + \Omega_U + \Omega_D) I_0(24.5^\circ)}{\Omega_F I_0(0^\circ)} \times \\ &\times \frac{[1 + \frac{1}{2} p_{zz} A_{zz}(24.5^\circ)]}{1 + \frac{1}{2} p_{zz} A'_{zz}(0^\circ)} \end{aligned} \quad (24)$$

With  $p_{zz} \ll 1, A_{zz} \sim 1$

$$\begin{aligned} &\frac{L_t + R_t + U_t + D_t}{F_t} \cong \frac{L + R + U + D}{F} \times \\ &\times \{1 + \frac{1}{2} p_{zz} [A_{zz}(24.5^\circ) - A'_{zz}(0^\circ)]\} \end{aligned} \quad (25)$$

i.e., if the beam acquires the tensor polarization in the target this should lead to a change in the ratio of the sum of the counts number of the side detectors to the counts of the forward detector.

The resulting energy dependence of the experimental points was approximated by a linear least-squares fit. The measurements were carried out with three different targets and the corresponding energies of the incident deuteron beam. The deuteron energies after the targets were found from the Bethe-Bloch formula and should be about 7 MeV. For example, a deuteron beam of 18.1 MeV in front of the carbon target with  $188 \frac{\text{mg}}{\text{cm}^2}$  produces 7 MeV average beam energy after the target. At this energy of the incident beam calibration measurements without a target were taken before.

For each target a similar processing of the spectrum was done. The thickness of each target and parameters of the linear fit for each case are shown in table I.

Experimental points for each target and related linear approximations are presented in Figs. 11-13. The sign  $\bullet$  mark experimental points  $(L+R+U+D)/F$  without a target (calibration) /  $\circ$

TABLE I: Thickness of targets and parameters of the linear fit.

Target thickness (mg/cm <sup>2</sup> )	Parameters of linear fit $y = kx + b$	
	$k$	$b$
0	-0.134 ± 0.005	1.72 ± 0.03
57.8 ± 1.0	-0.128 ± 0.005	1.68 ± 0.03
151 ± 3	-0.103 ± 0.006	1.50 ± 0.04
188 ± 4	-0.116 ± 0.005	1.59 ± 0.03

experimental points  $(L+R+U+D)/F$  for the targets of 58 mg/cm<sup>2</sup>, 151 mg/cm<sup>2</sup>, 188 mg/cm<sup>2</sup>, respectively / ······ the linear fit to experimental points  $(L+R+U+D)/F$  without target / — the linear fit to experimental points  $(L+R+U+D)/F$  for the targets of 58 mg/cm<sup>2</sup>, 151 mg/cm<sup>2</sup>, 188 mg/cm<sup>2</sup>, respectively, the line / - · - - corresponds to the tensor polarization  $p_{zz} = 0.1$ , which does not depend on the deuteron energy.

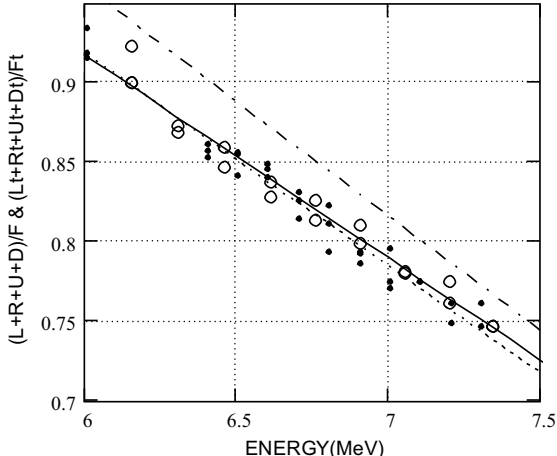


Fig. 11: Energy dependence of  $(L+R+U+D)/F$  without target and  $(L_t+R_t+U_t+D_t)/F_t$  for the target of 58 mg/cm<sup>2</sup> together with the corresponding linear approximations (● experimental points  $(L+R+U+D)/F$  without a target (calibration) / ○ experimental points  $(L+R+U+D)/F$  for the targets of 58 mg/cm<sup>2</sup>, 151 mg/cm<sup>2</sup>, 188 mg/cm<sup>2</sup>, respectively / ······ the linear fit to experimental points  $(L+R+U+D)/F$  without target / — the linear fit to experimental points  $(L+R+U+D)/F$  for the targets of 58 mg/cm<sup>2</sup>, 151 mg/cm<sup>2</sup>, 188 mg/cm<sup>2</sup>, respectively / - · - - the line corresponding to the tensor polarization  $p_{zz} = 0.1$ , which does not depend on the deuteron energy).

From the figures and the last table it is seen that straight lines for all cases considered do not coincide. Especially, it is evident for the targets of 151 mg/cm<sup>2</sup>

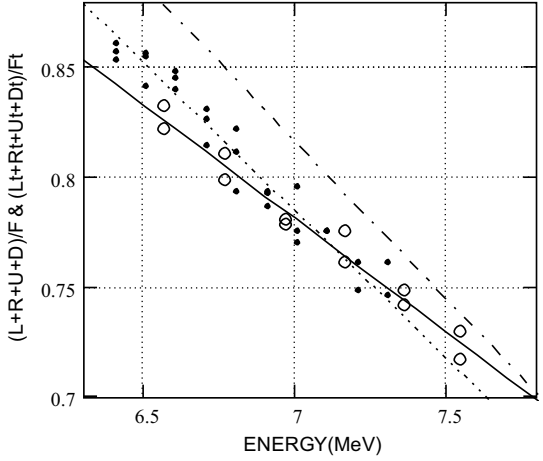


Fig. 12: Energy dependence of  $(L+R+U+D)/F$  without target and  $(L_t+R_t+U_t+D_t)/F_t$  for the target of 151 mg/cm<sup>2</sup> and the corresponding linear approximations (see Fig. 11).

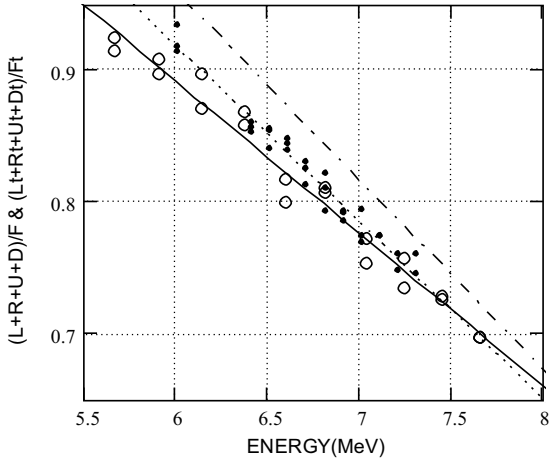


Fig. 13: Energy dependence of  $(L+R+U+D)/F$  without target and  $(L_t+R_t+U_t+D_t)/F_t$  for the target of 188 mg/cm<sup>2</sup> and the corresponding linear approximations (see Fig. 11).

and 188 mg/cm<sup>2</sup>, i.e. we have different tensor polarization (dichroism) for various target thickness. From the figures one more important conclusion follows: the straight line corresponding to tensor polarization 0.1 crosses the straight line corresponding to the unpolarized beam of deuterons with no target in the region of 16 MeV. Experimental data behave very differently, i.e. we have a rather strong dependence of the tensor polarization on the deuteron energy:

- Experimental points have a relatively wide spread with and without a target, although

with a target the influence of different focusing conditions should be smaller.

- Since the target thickness has an error of  $\pm 2\%$ , and there is no possibility to calibrate detectors, the error of the deuteron energy after the target obtained with the Bethe-Bloch formula and tables is  $\pm 0.2 \text{ MeV}$ . This means that the linear relation may be shifted in this interval for each target.

Therefore, a unique source of information about dichroism (tensor polarization arising) is the slope of the straight line which does not change essentially in this error interval, i.e. the change of line slope with and without a target testifies to dichroism (tensor polarization) arising according to (25). But since we do not know the deuteron energy after the targets exactly, we cannot find the difference between points on the lines corresponding to the same energy and analyzing power with sufficient accuracy. Though the magnitude of dichroism cannot be determined precisely by Eq. (25) within its errors yet from the slope we can conclude that dichroism exists and increases with energy in this energy region. The average dependence of dichroism on the deuteron energy after the target passage is shown in Figs.14-16 where the relation between tensor polarization and dichroism is used:  $A = -\frac{3}{4}p_{zz}$ .

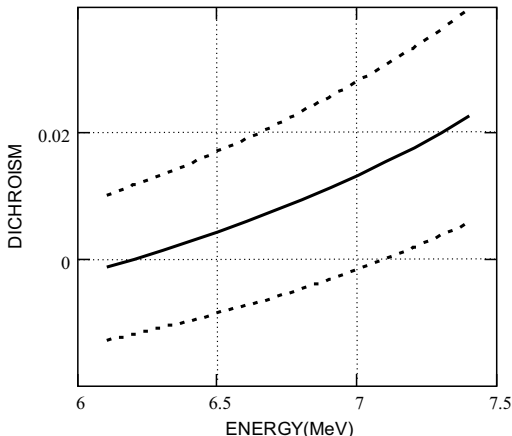


Fig. 14: Dependence of dichroism on the deuteron energy after the passage of a carbon target of  $58 \text{ mg/cm}^2$  ( - - - range of deviation).

## VI. CONCLUSION

According to experimental results it is possible to draw the following conclusions:

1. For all three carbon targets spin dichroism of deuterons is observed, especially visible for the

targets of  $151 \text{ mg/cm}^2$ ,  $188 \text{ mg/cm}^2$ .

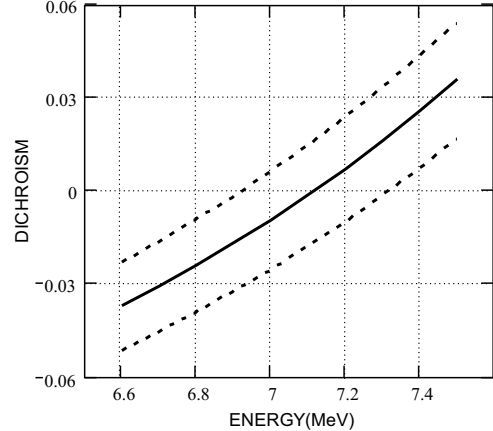


Fig. 15: Dependence of dichroism on the deuteron energy after the passage of a carbon target of  $151 \text{ mg/cm}^2$  (see Fig. 14).

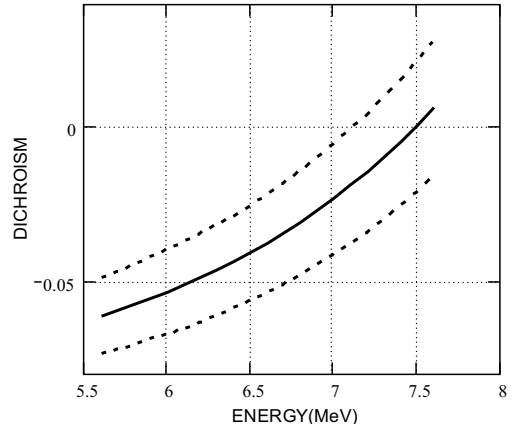


Fig. 16: Dependence of dichroism on the deuteron energy after the passage of a carbon target of  $188 \text{ mg/cm}^2$  (see Fig. 14).

2. Dichroism grows in the energy region 6-20 MeV.
3. The sign change of spin dichroism and its not being proportional to the target thickness can be explained by a more complicated dependence of the cross section on the energy of particles, which changes when the beam passes through the target. For a more complete description of the dichroism observed in this energy region it is necessary to take into account spin-spin and Coulomb interactions and a possible influence of resonant reactions of deuterons with carbon.

- 
- [1] V. Baryshevsky, M. Podgoretsky, *Zh. Eksp. Theor. Fiz.* 47 (1964) 1050.
- [2] A. Abragam et al., *C.R. Acad. Sci.* 247 (1972) 423
- [3] M. Forte, *Nuovo Cim. A* 18 (1973) 727.
- [4] A. Abragam, M. Goldman, *Nuclear Magnetism: order and disorder* (Oxford Univ. Press, Oxford, 1982).
- [5] V. Baryshevsky, *Phys. Lett. A* 171 (1992) 431.
- [6] V. Baryshevsky, *J. Phys. G* 19 (1993) 273.
- [7] V. Baryshevsky, F. Rathmann, Oscillation and rotation of deuteron spin in polarized and unpolarized targets, COSY summer school, Vol.1 (2002).
- [8] S. Kox et al.; *Nucl. Instr. and Meth.* **A346** (1994) 527.
- [9] F. J. M. Farley, K. Jungmann, J. P. Miller, W.M. Morse, Y. F. Orlov, B. L. Roberts, Y. K. Sermartzidis, A. Silenko, and E. J. Stephenson, *Phys. Rev. Lett.* Vol. 93 N. 5 (30 July 2004).
- [10] V. Baryshevsky, K. Batrakov, S. Cherkas, arXiv:hep-ph/9907464 v1 (23 Jul 1999).
- [11] D. Varshalovich, A. Moskalev, V. Khersonsky, *Quantum theory of angular momentum*, Moscow, Science 1975, p.46 (in Russian).
- [12] G. G. Ohlsen, Polarization transfer and spin correlation experiments in nuclear physics, *Rep. Prog. Phys.* 35 (1972) 717.
- [13] Diploma thesis, R. Engels, Institut für Kernphysik, Universität zu Köln (1997) <http://www.ikp.uni-koeln.de/~3T/arbeiten/engels.diplom.ps.gz>.(in German).
- [14] M. Bittcher, W. Grüebler, V. König, P.A. Schmelzbach, B. Vuaridel und J. Ulbricht; *Few-Body Sys.* **9** (1990) 165.